Supplementary material

Textile-based triboelectric nanogenerator with alternating positive and negative freestanding grating structure

Watcharapong Paosangthong[a,*], Mahmoud Wagih[a], Russel Torah[a], Steve Beeby[a]

[a]*School of Electronics and Computer Science, University of Southampton, Southampton, SO171BJ, UK*

**Corresponding author*

E-mail addresses: wp1y15@soton.ac.uk (W. Paosangthong), mahm1g15@soton.ac.uk (M. Wagih), rnt@ecs.soton.ac.uk (R. Torah), spb@ecs.soton.ac.uk (S. Beeby)

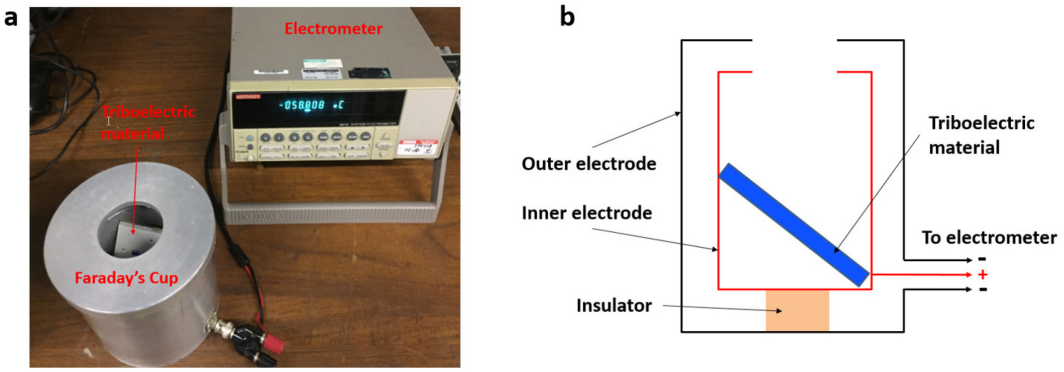

Fig. S1. Surface charge density measurement system. (a) Photograph of Faraday's cup connected to an electrometer and (b) schematic illustration of Faraday's cup.

To measure the surface charge density of the triboelectric materials, the triboelectric materials were rubbed against the electrodes using the linear actuator at an oscillation frequency of 2 Hz, a travel distance of the lower substrate of 46 mm and a contact force of 5 N. The V_{OC} of the TENGs were monitored using the oscilloscope. When the V_{OC} has saturated at its maximum value, the triboelectric materials were immediately put in a Faraday's cup which was connected to an electrometer (Keithley 6514), shown in Fig.S1(a). The Faraday's cup is composed of an inner and outer conductive cup, which serves as an inner and outer electrode, shown in Fig. S1(b). The inner cup is connected to the electrometer and is separated from the outer cup by an insulator. When the charged triboelectric material is put into the inner cup, the same quantity of charges with the opposite polarity will be transferred from the outer cup through the electrometer to the inner cup. The number of the transferred charges is equal to the total number of the charges on the surface of the triboelectric material and can be measured via the electrometer.

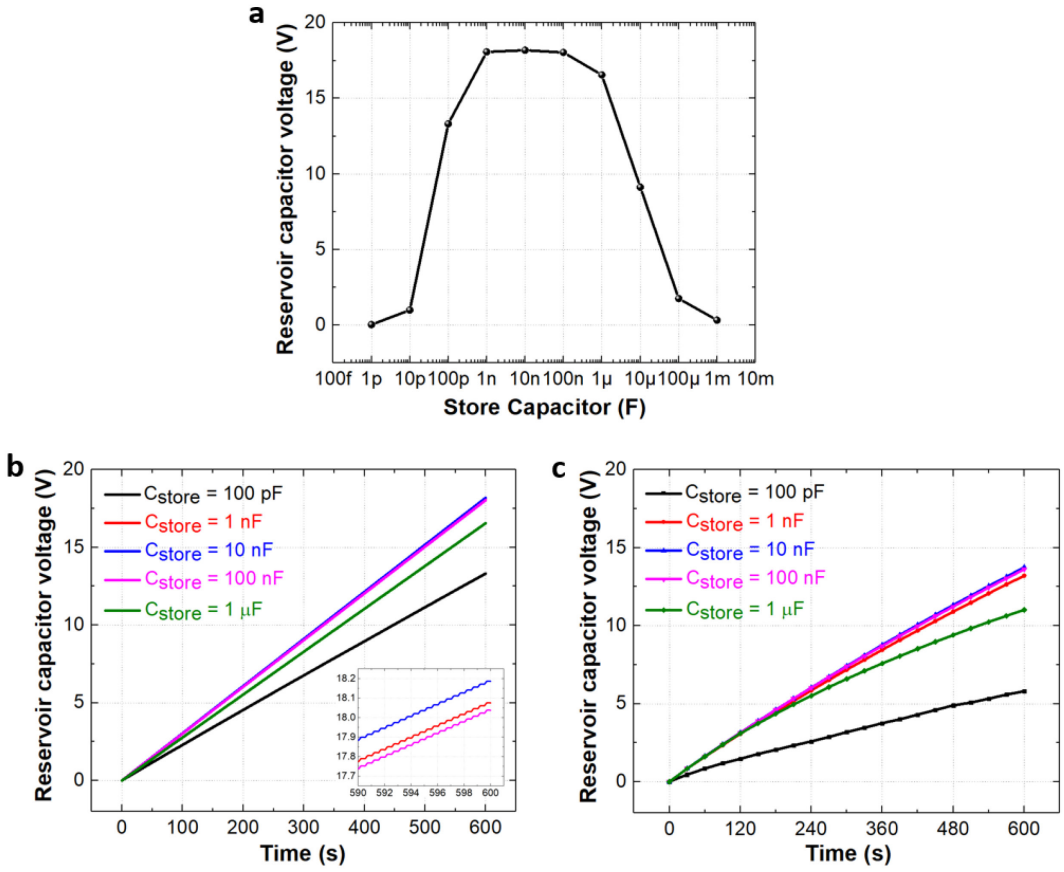

Fig. S2. (a) Simulated maximum V_C after a charging time of 600 s as a function of C_{store}. (b) Simulated transient V_C of Bennet's doubler circuit for the different C_{store}. The inset shows the magnified V_C for C_{store} = 1, 10 and 100 nF at the time between 590 and 600 s. (c) Experimental transient V_C of Bennet's doubler circuit for the different C_{store}.

The simulated maximum reservoir capacitor voltage (V_C) for the Bennet's doubler circuit at a charging time of 600 s as a function of capacitance of the store capacitor (C_{store}) is revealed in Fig. S2a. The maximum V_C rises sharply with increasing C_{store} for the C_{store} smaller than 1 nF. Next, it stays almost constant for the C_{store} between 1 nF and 100 nF, then decreases rapidly when the C_{store} exceeds 100 nF. The maximum V_C peaks at a value of 18.19 V for C_{store} = 10 nF. Fig. S2b shows that the simulated V_C increases with time for all C_{store} and reaches maximum values of 13.31 V, 18.08 V, 18.19 V, 18.04 V and 16.55 V for C_{store} = 100 pF, 1 nF, 10 nF, 100 nF and 1 µF, respectively. The experimental transient V_C of the TENG connected to the Bennet's doubler circuit for various C_{store} are presented in Fig. S2c. The maximum V_C of 13.75 V is obtained for C_{store} = 10 nF at a charging time of 600 s, followed by those for C_{store} = 100 nF, 1 nF, 1 µF and 100 pF. Compared to the simulation results, the sequence of the maximum V_C for the different C_{store} and the different rectifier circuits are in good agreement. The values of the V_C in the real operation are lower than the simulation result due to losses in the circuits, such as resistive loss.

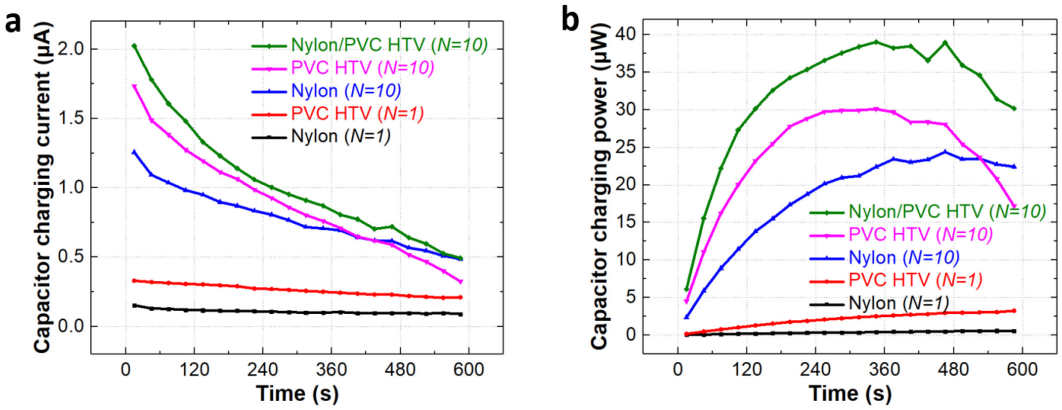

Fig. S3. (a) Calculated capacitor charging current (I_C) and (b) Calculated capacitor charging power (P_C) as a function of time for different types of TENGs.

The transient capacitor charging current I_C (Fig. S3a) is calculated from the V_C (Fig. 6c) using Eq. (1) below:

$$I_C = \frac{\Delta Q}{\Delta t} = \frac{C \cdot \Delta V_C}{\Delta t} \tag{1}$$

where ΔQ is the transferred charge during a charging time Δt of 30 s, ΔV_c is the change in V_c between a charging time Δt of 30 s and C is the capacitance e.g. 10 μF. The I_C decreases over time for all TENGs. The pnG-TENG produces the maximum I_C of 2.02 μA, followed by the pG-TENG, the nG-TENG and the TENGs with no grating. The reason of the reduction in I_C over time is due to the growth in V_C and the increase in the stored charge in the capacitor, reducing the movement of electrons. The transient capacitor charging power (P_C) (Fig. S3b) is also calculated from the V_C (Fig. 6c) using Eq. (2) below:

$$P_C = \frac{\Delta E}{\Delta t} = \frac{\frac{1}{2}C({V_{C,2}}^2 - {V_{C,1}}^2)}{\Delta t} \tag{2}$$

where ΔE is the change in capacitor energy between a charging time Δt of 30 s. The P_c of the pnG-TENG reaches the maximum value of 39.0 μW, with the P_c of the other TENGs in the same peak performance sequence as the two previous graphs.

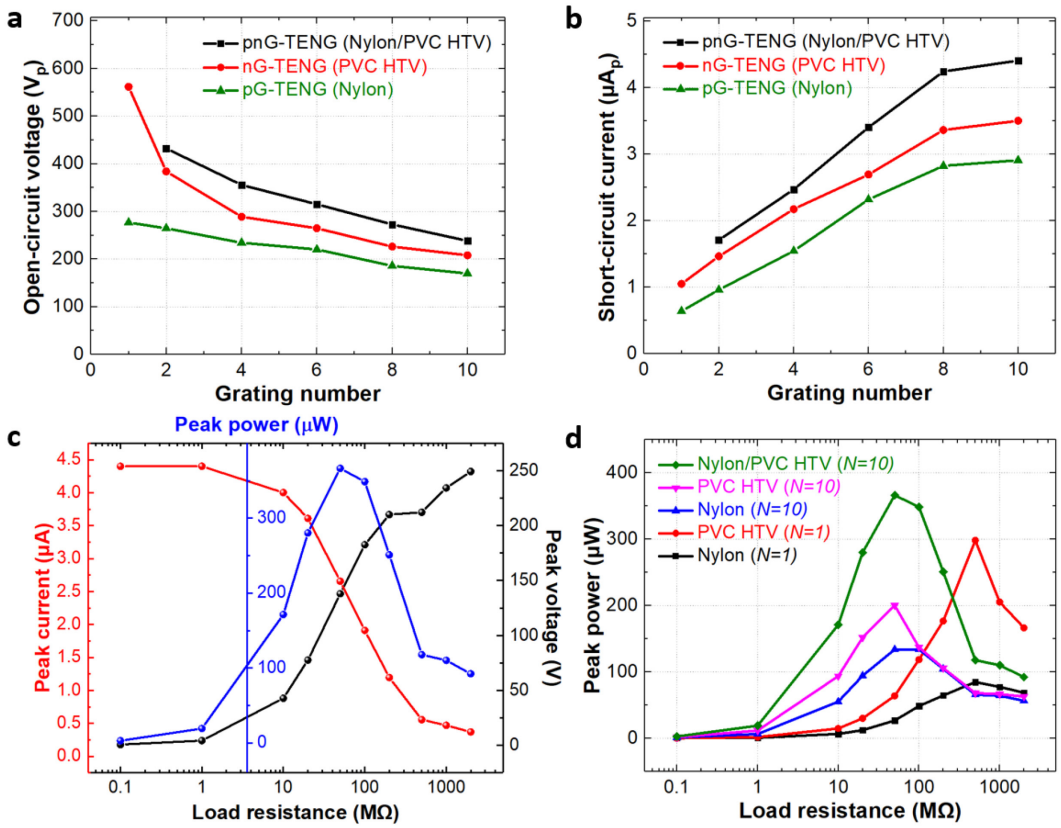

Fig. S4. The zero to peak values of (a) V_{OC} and (b) I_{SC} as a function of grating number for the different types of TENGs. (c) The dependence of the V_{pk}, I_{pk} and P_{pk} on the external load resistance for the pnG-TENG (Nylon/PVC HTV, $N = 10$). (d) Load-dependent P_{pk} for the different types of TENGs.

The zero to peak value of V_{OC} and I_{SC} are represented in Fig. S4a and S4b, respectively. In good accordance with the RMS values, the V_{OC} decreases with increasing grating number for all types of TENGs, whereas the I_{SC} grows up. Compared to the nG-TENGs and the pG-TENGs, the outputs of the pnG-TENGs are enhanced for all grating numbers. The peak voltage (V_{pk}), peak current (I_{pk}) and peak power (P_{pk}) as a function of the external load for the pnG-TENG (Nylon/PVC HTV, $N = 10$) are illustrated in Fig. S4c. The V_{pk} rises with increasing load resistance, then remains constant and reaches a V_{OC} of 238 V, while the I_{pk} shows a reversed tendency. It starts from an I_{SC} of 4.41 μA, then drops to zero at very large resistance. The pnG-TENG produces the maximum P_{pk} of 366 μW at a load resistance of 50 MΩ, corresponding to a peak power density of 114 mW/m^2. The P_{pk} for the different types of TENGs are compared in Fig. S4d. At a load resistance of 50 MΩ, the pnG-TENG (Nylon/PVC HTV, $N = 10$) generates the highest P_{pk}, followed by the nG-TENG (PVC HTV, $N = 10$), the pG-TENG (Nylon, $N = 10$), the TENG with no grating (PVC HTV, $N = 1$) and the TENG with no grating (Nylon, $N = 1$).

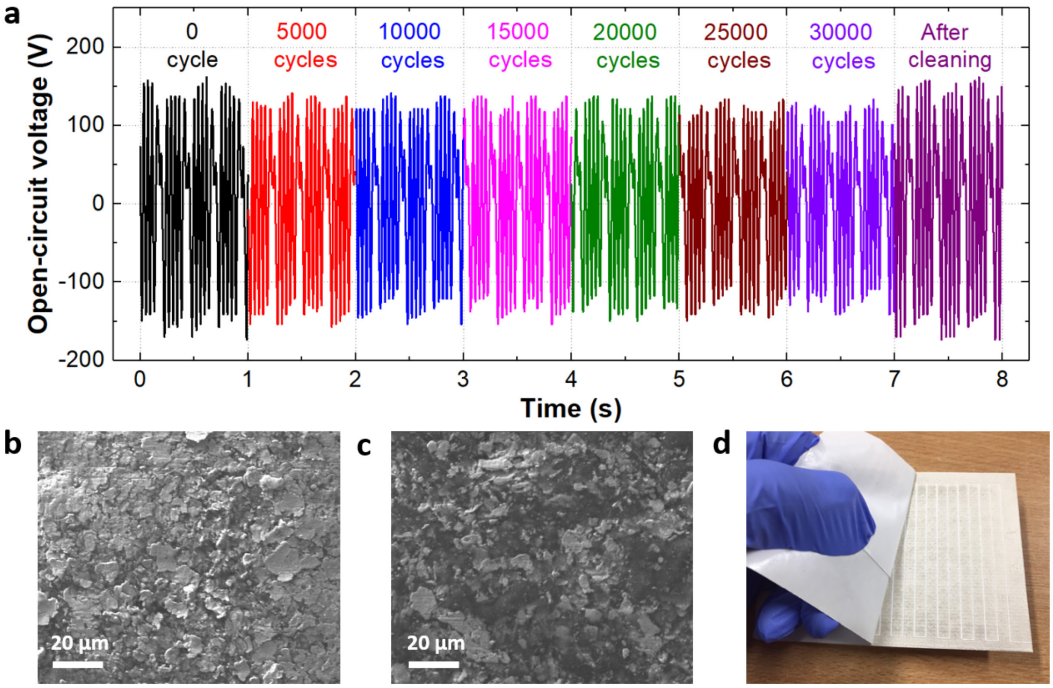

Fig. S5. (a) Transient V_{OC} of pnG-TENG for the different operating cycles. SEM images of Ag IDE (b) before and (c) after stability test. (d) Photograph of an adhesive tape test during which the tape does not pick up any material.

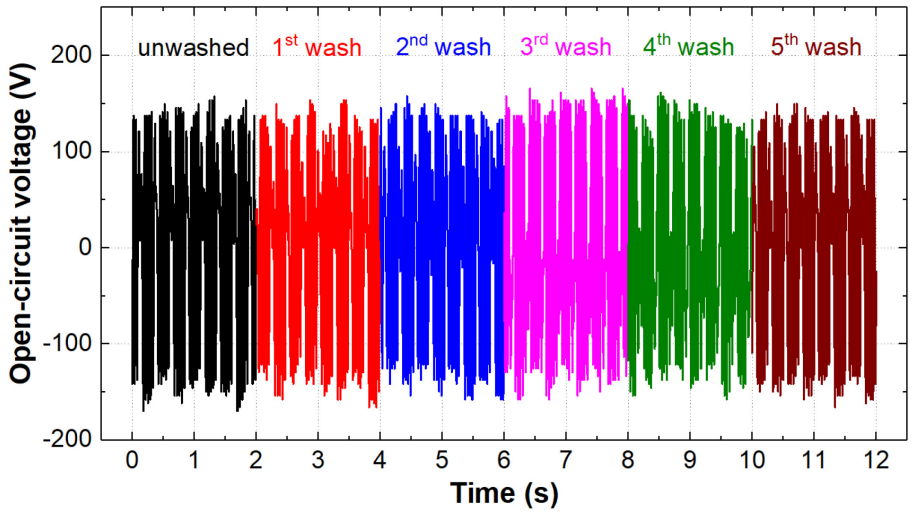

Fig. S6. Transient V_{OC} of pnG-TENG for the different washing cycles.

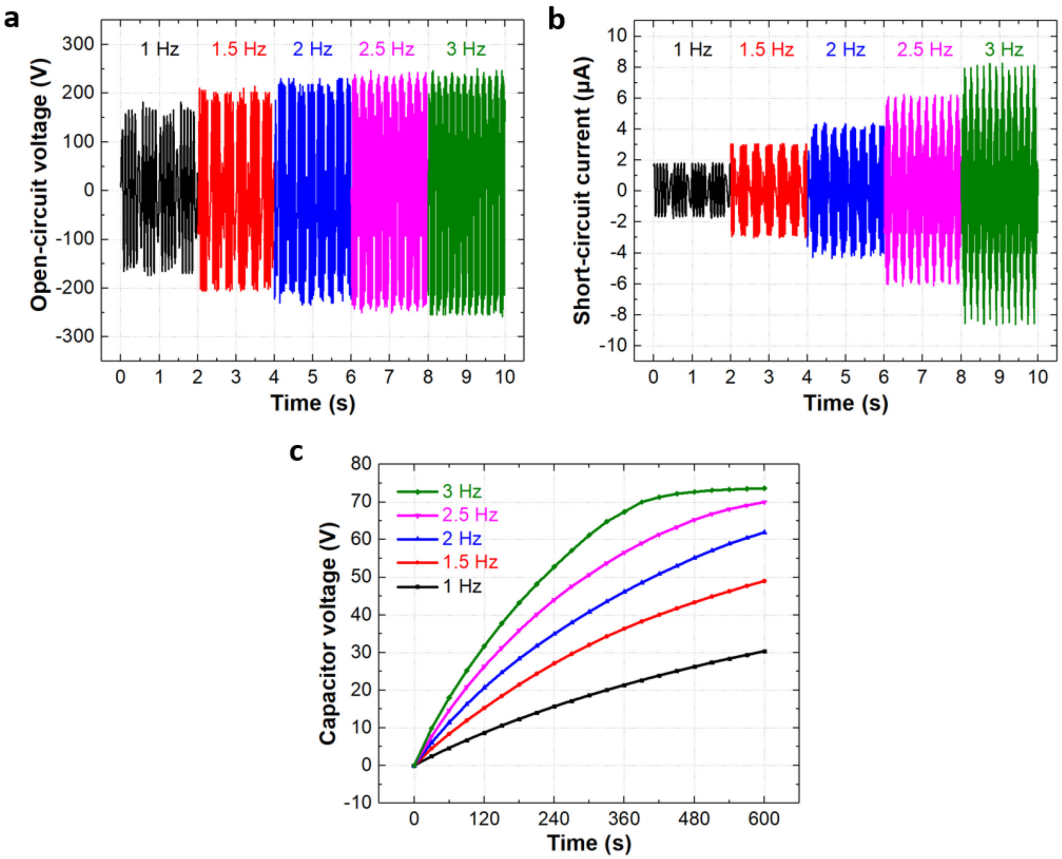

Fig. S7. Transient (a) V_{OC} and (b) I_{SC} and (c) V_C of the pnG-TENG (Nylon/PVC HTV, $N = 10$) for the different frequencies.

The transient V_{OC} and I_{SC} of the pnG-TENG with nylon fabric and PVC HTV ($N = 10$) for different frequencies are demonstrated in Fig. S7a and S7b, respectively. The V_{OC} increases with increasing frequency and saturates for the frequency over 2.5 Hz, whereas the I_{SC} shows a linear growth with increasing frequency. The corresponding transient V_C is shown in Fig. S7c. The slope of the V_C curve grow up with a larger frequency. At a frequency of 3 Hz, the V_C reaches 73.6 V at a charging time of 600 s.

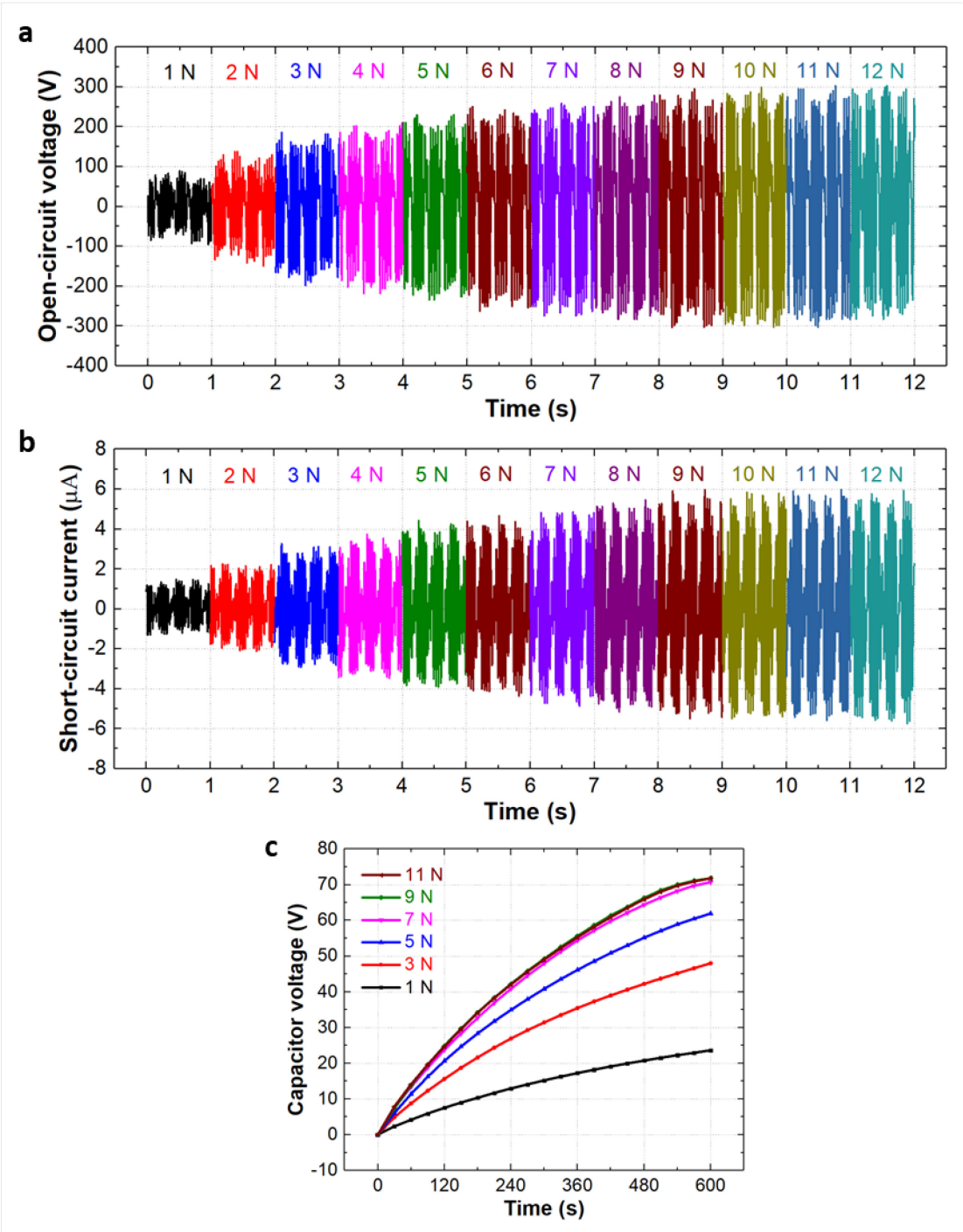

Fig. S8. Transient (a) V_{OC} and (b) I_{SC} and (c) V_C of the pnG-TENG (Nylon/PVC HTV, $N = 10$) for the different contact forces.

The transient V_{OC} and I_{SC} of the pnG-TENG (Nylon/PVC HTV, $N = 10$) for various contact forces are illustrated in Fig. S8a and S8b. They increase with increasing contact force and then saturate at the contact force over 9 N. The time-dependent V_C for the different contact force, shown in Fig. S8c, confirms that the V_C reaches a saturation point at a contact force of 9 N with a maximum V_C of 71.8 V at a charging time of 600 s.

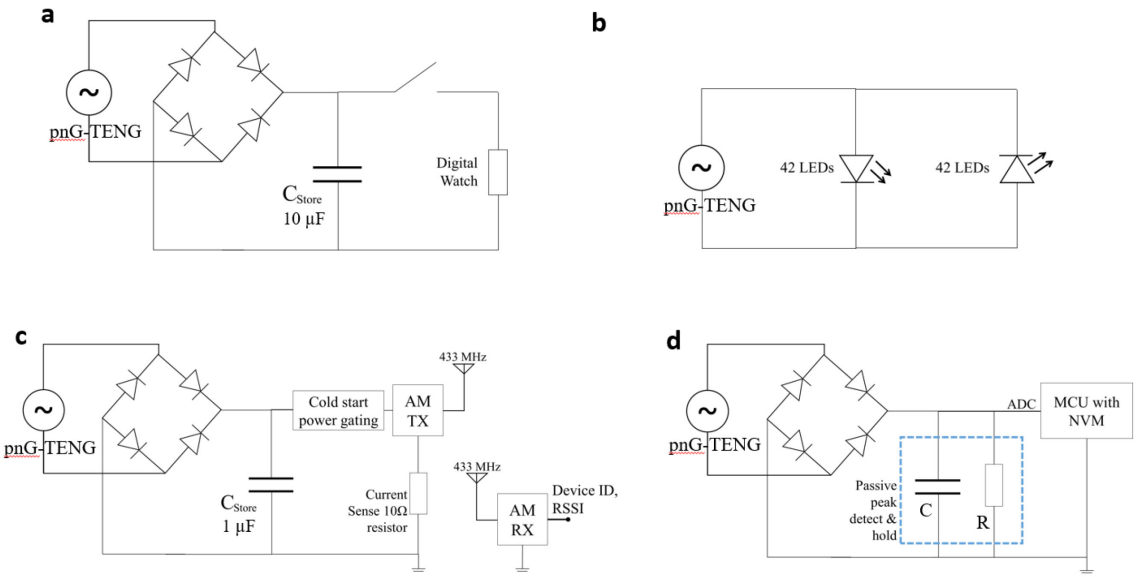

Fig. S9. Circuit diagrams of using pnG-TENG for powering (a) a digital watch, (b) night-time warning indicator, (c) wireless transmitter and (d) pedometer.

Video 1: Driving a digital watch using the output of the pnG-TENG when running.

Video 2: Driving a wearable night-time warning indicator for pedestrians using the output of the pnG-TENG when running.

Video 3: Using the output signal of the pnG-TENG as a trigger signal for pedometer when walking.